Recent advances in geosynthetic-reinforced retaining walls for highway applications

Article *in* Frontiers of Structural and Civil Engineering · August 2017

DOI: 10.1007/s11709-017-0424-8

3 authors, including:

Jie Han
University of Kansas
343 PUBLICATIONS **5,424** CITATIONS

SEE PROFILE

Yan Jiang
Terracon Consultants, Inc.
19 PUBLICATIONS **146** CITATIONS

SEE PROFILE

Front. Struct. Civ. Eng. 2018, 12(2): 239–247
DOI 10.1007/s11709-017-0424-8

REVIEW

Recent advances in geosynthetic-reinforced retaining walls for highway applications

Jie HAN[a*], Yan JIANG[b], Chao XU[c]

[a] *Department of Civil, Environmental, and Architectural Engineering, University of Kansas, Lawrence, KS 66044, USA*

[b] *Terracon Consultants, Inc., 2201 Rowland Ave, Savannah, Georgia 31404, USA*

[c] *Department of Geotechnical Engineering, College of Civil Engineering, Tongji University, Shanghai 200092, China*

[*] *Corresponding author. E-mail: jiehan@ku.edu*

ABSTRACT Geosynthetic-reinforced retaining (GRR) walls have been increasingly used to support roadways and bridge abutments in highway projects. In recent years, advances have been made in construction and design of GRR walls for highway applications. For example, piles have been installed inside GRR walls to support bridge abutments and sound barrier walls. Geosynthetic layers at closer spacing are used in GRR walls to form a composite mass to support an integrated bridge system. This system is referred to as a geosynthetic-reinforced soil (GRS)-integrated bridge systems (IBS) or GRS-IBS. In addition, short geosynthetic layers have been used as secondary reinforcement in a GRR wall to form a hybrid GRR wall (HGRR wall) and reduce tension in primary reinforcement and facing deflections. These new technologies have improved performance of GRR walls and created more economic solutions; however, they have also created more complicated problems for analysis and design. This paper reviews recent studies on these new GRR wall systems, summarizes key results and findings including but not limited to vertical and lateral earth pressures, wall facing deflections, and strains in geosynthetic layers, discusses design aspects, and presents field applications for these new GRR wall systems.

KEYWORDS bridge, geosynthetic, highway, reinforced, wall

1 Background

Geosynthetic-Reinforced Retaining (GRR) walls have been increasingly used to support roadways and bridge abutments in highway projects (e.g, Refs. [1–6].). The GRR walls mainly consist of wall facing, compacted backfill material, and geosynthetic reinforcement. Fig. 1(a) shows a typical cross section of the GRR wall with a modular block facing. During construction of the GRR wall, geosynthetic reinforcement is installed between layers of compacted backfill to provide tensile resistance. Frictional or mechanical connections are commonly used to connect geosynthetics with the wall facing. In addition to modular blocks, concrete panels and wrapped-around geosynthetics have been used for the wall facing.

Design of GRR walls typically considers external, internal, and local stability [7,8]. Fig. 1(b) shows the force diagram of a GRR wall. For an external stability analysis, the reinforced mass of the GRR is often treated as a rigid body. The external force, $P_{a(ext)}$, from the retaining soil, is considered as a driving force. The weight of the reinforced mass, W, and the friction at the bottom of the reinforced mass, Q, are the resisting forces. Higher resisting forces than the driving force with a certain factor of safety are needed to ensure the external stability against sliding and overturning of the reinforced mass. In addition, the foundation soil should have sufficient bearing capacity to prevent the bearing failure. Within the reinforced mass, the internal earth pressure, $p_{a(int)}$, is applied to the wall facing, which is carried by the tensile forces from the geosynthetic layers. A potential failure plane, often assumed as the Rankine or Coulomb failure plane, is used to define active and stable zones. To ensure the safety of the geosynthetic layers, they should have sufficient tensile strengths and pullout capacities. The pullout capacity of each geosynthetic layer depends on the normal

Article history: Received Dec 4, 2016; Accepted Jan 28, 2017

stress, q_r, the anchorage length in the stable zone, and the interface properties between the geosynthetic and the soil. In addition to external and internal stability, local stability at wall facing is important. To avoid local facing bulging, AASHTO [7] suggested that the maximum reinforcement spacing should be limited to twice the block width if modular blocks are used for wall facing. For typical GRR walls, the reinforcement spacing is equal or larger than 0.3 m and the maximum reinforcement spacing is 0.6 m. In addition to reinforcement spacing, sufficient connection strength between each geosynthetic layer and wall facing is needed.

In recent years, advances have been made in construction and design of GRR walls for highway applications. For example, piles have been installed inside GRR walls to support bridge abutments and sound barrier walls [4,9–12]. Geosynthetic layers at closer spacing (smaller than 0.3 m) are used in GRR walls to form a composite mass to support an integrated bridge system [13–20]. This system is also referred to as the geosynthetic-reinforced soil (GRS)-integrated bridge systems (IBS) or GRS-IBS. In addition, short geosynthetic layers have been used as secondary reinforcement with closer spacing (smaller than 0.3 m) in the GRR wall to form a hybrid GRR wall and reduce tension in primary reinforcement layers and facing deflections [6,21–25]. Fig. 2 presents the above applications of GRR walls. These technologies have improved the performance of GRR walls and created more economic solutions; however, they have also created more complicated problems for analysis and design.

This paper reviews recent studies on these GRR wall systems, summarizes key results and findings including but not limited to vertical and lateral earth pressures, wall facing deflections, and strains in geosynthetic reinforcements, discusses design aspects, and presents field applications for these new GRR wall systems.

2 Piles in GRR walls

A laterally loaded pile installed in a GRR wall is usually designed to have an isolation casing throughout the reinforced soil and have a socket into an underlying stable foundation. This design eliminates the interaction between

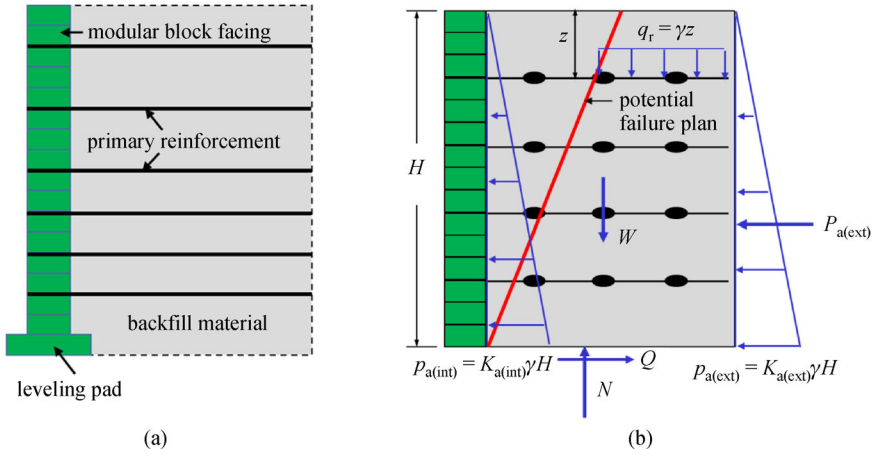

Fig. 1 Cross section and force diagram of a GRR wall. (a) Cross section and components; (b) Force diagram and stability analysis

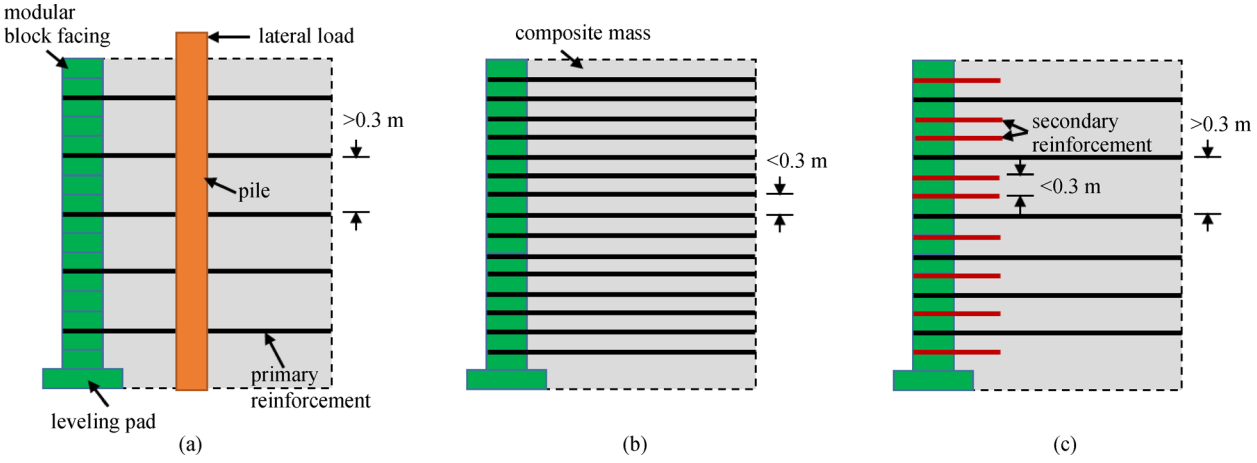

Fig. 2 Recent applications of GRR walls. (a) Pile in GRR wall; (b) GRS wall; (c) Hybrid GRR wall

the pile and the GRR wall but results in a large diameter pile and a required socket, which are expensive. Pierson et al. [4,9,26] performed a series of field tests to study the behavior of laterally-loaded piles directly installed in a GRR wall without any isolation casing and socket. Fig. 3 shows a typical cross section of the GRR wall and the lateral pile load test setup. These tests evaluated lateral load capacities and deflections of a single pile and group piles in the GRR wall as well as the performance of the GRR wall when piles were laterally loaded.

The tested GRR wall was constructed on a limestone foundation and had 42 m in length and 6 m in height. The wall facing was comprised of stacked modular blocks and used mechanical connectors to connect facing blocks with geogrids. Ten layers of geogrids were used, which included four strong layers in the lower portion and six weak layers in the upper portion. The length of geogrids was 4.2 m (0.7 times the wall height) and vertical reinforcement spacing was 0.6 m. Backfill material was clean aggregate with a peak friction angle of 51° from triaxial tests. Eight tested piles without sockets and six reaction piles with sockets into the limestone foundation were constructed, respectively. The tested piles had a diameter of 0.9 m and seven of them were cast in place from the bottom of the wall and one was cast in place from 1.5 m above the bottom of the wall. The wall had one meter embedment. The tested piles were laterally loaded toward the wall facing. Instrumentation, which included inclinometer casings, load cells, linear variable differential transformers (LVDTs), earth pressure cells, and foil-type strain gauges, was installed to monitor the performance of the piles and the wall. In addition, a photogrammetry technique was adopted to monitor the wall facing deflections during each loading test. The deflections along the pile, the applied lateral load, and the displacement on the pile head were measured to evaluate the behavior of the tested pile. The wall facing deflections,

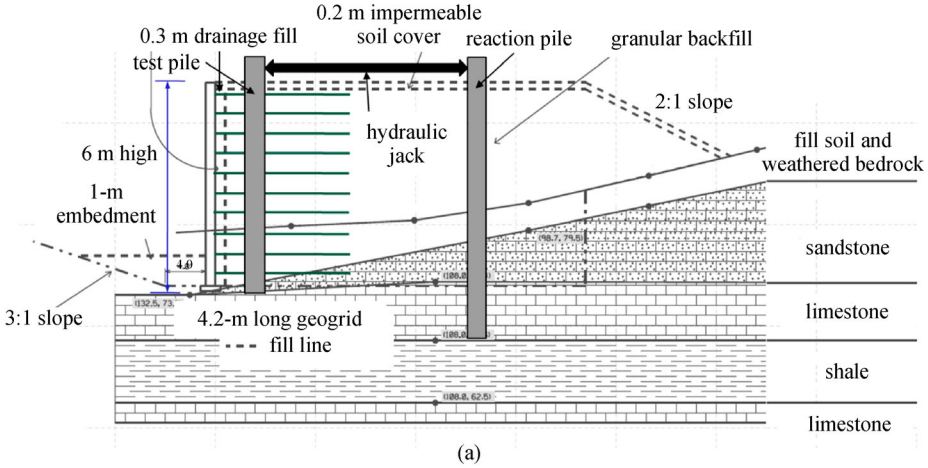

(a)

(b)

Fig. 3 Field test of a laterally loaded pile in a GRR wall. (a) Cross section; (b) Top view of setup for a single pile test

the lateral earth pressures behind the wall facing, and the strains in geogrids were measured to evaluate the performance of the wall.

Fig. 4 shows the lateral load-displacement relationships of the pile heads with the single and group piles at different distances (1*D*, 2*D*, 3*D*, and 4*D*, *D* is the pile diameter) away from the wall facing. Fig. 4 shows the displacement of the pile head increased with an increase in the applied lateral load. To reach the same displacement, the tested pile at the larger distance away from the wall facing required more lateral load on the pile. In addition, the group piles with pile spacing of 4.5 m deflected more than a single pile when the piles were located at two times the pile diameter (2*D*) from the facing. The reduction in the lateral load capacity of the group piles resulted from the pile group effect and should be considered in design. Fig. 5 illustrates this group effect within the GRR wall. There is an influence width of each pile in the pile group. The width of influence of a pile causing a group effect depends on the distance from the center of the pile to the back of the wall facing.

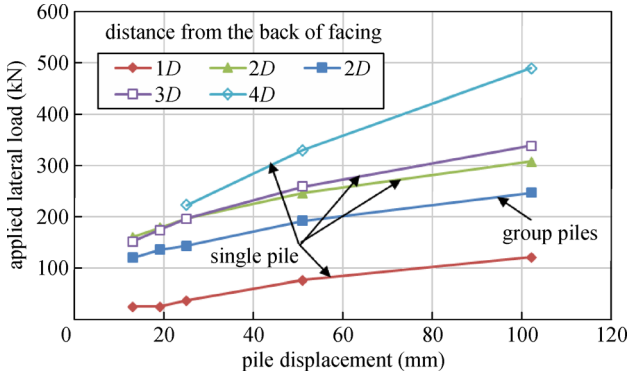

Fig. 4 Final load versus pile displacement with pile at different distance from the back of wall facing (modified from Pierson et al., 2008 [9])

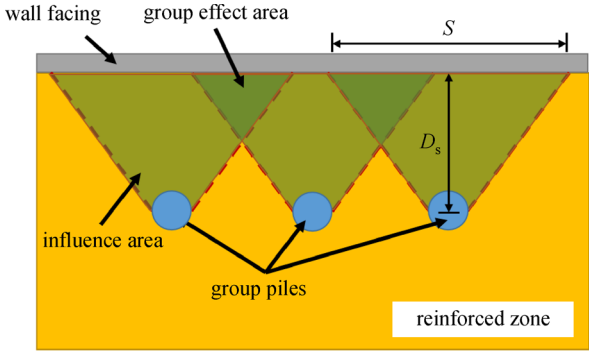

S: minimum pile spacing to prevent group effect
D_s: distance from the back of facing to the center of pile

Fig. 5 Illustration of pile group effect within a GRR wall

Before and after the field tests performed by Pierson et al. [4,9], the pre-test and post-test numerical studies were conducted by Huang et al. [12] to predict and evaluate the performance of piles and the GRR wall using a three-dimensional numerical software based on a finite differential method. In their numerical model, the backfill material, the retained soil, and the grade soil were modelled as linearly elastic-perfectly plastic materials with the Mohr-Coulomb failure criteria while the foundation soil, the pile, the wall facing, and the geogrids were modeled as elastic materials. Only an interface between pile and backfill material was considered in the numerical model. The numerical results show that the pre-test and post-test numerical simulation generally predicted the lateral earth pressures at the back of facing as well as the shape of the wall deflection in vertical and horizontal directions. Huang et al. [11] refined the numerical modeling to simulate the laterally-loaded pile in the GRR wall as shown in Fig. 6(a). In this refined model, an advanced soil constitutive model referred to as the Cap-Yield model was used to describe the behavior of the backfill material. The Cap-Yield model can characterize the compression and shear hardening/softening behavior of reinforced backfill. This advanced model is capable of

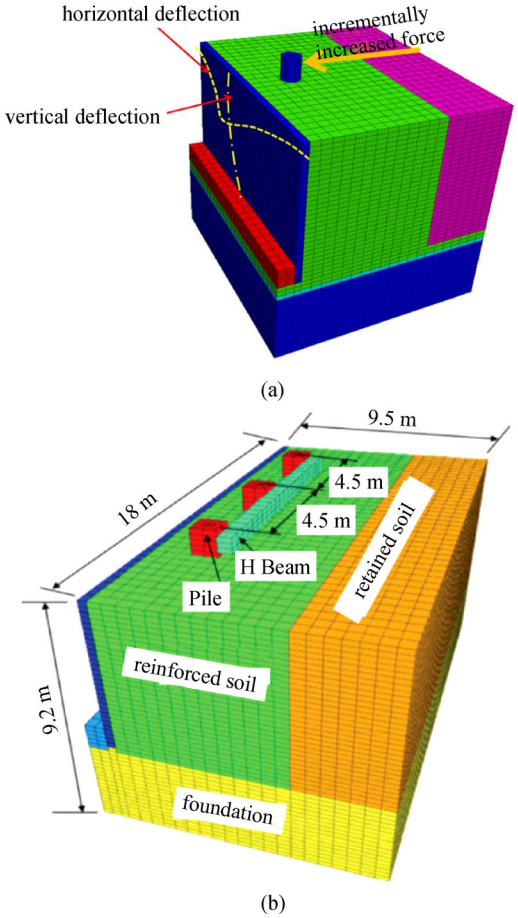

Fig. 6 Numerical modelling of single and group piles in the GRR wall (after Huang et al. [10,11]). (a) Single pile load test; (b) Group pile load test

accounting for both shear and compression yielding. Interfaces between block and block, between block and backfill material, and between reinforcement layers and backfill material, and a compaction stress were also considered. The measured and numerical results show that the vertical deflections of the wall facing increased with the wall height and the maximum deflection occurred at the wall top. The deflection of the wall facing at the bottom of wall was small due to a restraint from a grade soil in front of the wall as well as that of the pile at the bottom. In addition, the lateral earth pressure at the back of facing increased with the lateral load on the pile, which led to the state of lateral earth pressures ranging between the states of at-rest and passive earth pressure. The lateral load on the pile resulted in an increase of lateral earth pressure in the central region of the wall and a decrease in the adjacent region. Huang et al. [10] developed another numerical model with the same constitutive models for the materials used in Huang et al. [11] to assess the behavior of group piles in the GRR wall as shown in Fig. 6(b) and found that the strains in the geogrids reached to the maximum values around the piles. The influence of the friction angle of the backfill material and the tensile stiffness of the geogrids was not significant on the group effect but the modulus of backfill material had a significant influence on the group effect.

3 Geosynthetic-reinforced soil (GRS) walls

A GRR wall with closer reinforcement is also regarded as the GRS wall. A typical reinforcement spacing in GRR walls is 0.6 m while the spacing in GRS walls is smaller than 0.3 m. The GRS walls are often constructed as abutments to support small and medium-size bridges. Wu et al. [14] reported and summarized the existing in-service GRS walls with flexible facing to support bridges. Adams et al. [27] published a manual to design a GRS wall supporting an integrated bridge system. This system is referred to as a geosynthetic-reinforced soil (GRS)-integrated bridge systems (IBS) or GRS-IBS. Fig. 7 presents a typical cross section of the GRS-IBS. This new system includes a GRS wall and an integrated bridge system above the GRS wall. A maximum vertical spacing of geosynthetic reinforcement at smaller than 0.3 m in GRS walls is recommended. Wu [13] stated that the benefit of geosynthetic reinforcement was significantly enhanced with vertical spacing of reinforcement smaller than 0.3 m. Up to 2015, there are more than 200 bridges that were built using GRS abutments in the United States. Fig. 8 shows a GRS-IBS constructed in Colorado, USA with locally available natural rock blocks as the wall facing. Woven geotextile layers were placed between these rock blocks without any mechanical connection. This application demonstrates that connection force is low in the GRS wall.

Field tests have been conducted on the GRS structures including the GRS piers, the GRS abutments, and the GRS-IBS. Most of these GRS structures used modular-block facing while few used wrapped-around facing. GRS wall heights varied from 1.14 to 6.81 m and woven geotextile was the most commonly used reinforcement except one structure using geogrid as reinforcement [19]. Various types of backfill materials were used to construct the GRS walls, including well-graded gravel, silty sand with clay, and coarse aggregate. A reinforced foundation encapsulated with geotextile was also commonly adopted

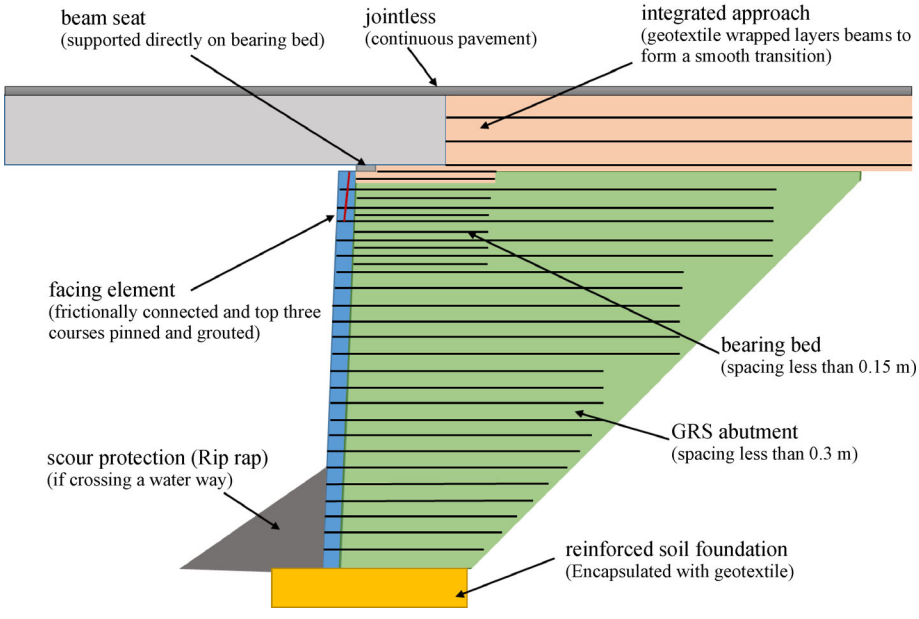

Fig. 7 Cross section of the GRS-IBS system (re-drawn from Adams et al. [27])

Fig. 8 Constructed GRS wall with natural rock blocks as facing

in these GRS structures. In addition, under the bridge beam, a bearing bed with even closer reinforcement spacing (smaller than 0.15 m) was used. In these field tests, instrumentation, including inclinometer casings, earth pressure cells, strain gauges, and surveying, was employed to monitor the behavior of these GRS structures, such as settlement, lateral deformation, and vertical and lateral earth pressures.

Wu [13] reported a field test of a GRS pier in Turner Fairbank, Virginia in the United States. The pier was constructed on a three-layer geogrid-reinforced foundation. A footing load seated on the top of the pier was loaded up to 900 kPa with seven stages. The measured vertical deformation of the pier approximately linearly increased with an increase of applied footing pressure up to 825 kPa and dramatically increased after 825 kPa, which indicated the ultimate bearing capacity of this pier. The lateral deformation of the wall facing also increased with the applied footing load. The maximum lateral deformation of the wall facing first happened in the upper part of the wall and then moved to the middle of the wall height with an increase of the footing load. A clear bulge was found in the middle area of the wall facing when the footing load reached to the ultimate bearing capacity. In addition, the measured strains in reinforcement increased with the applied footing load to 2.3% when the applied footing pressure was 900 kPa. The measured strains in each instrumented geotextile were uniformly distributed because the footing load was evenly applied over the entire area of the pier. The maximum strains in the geotextiles occurred in the area near the middle of the wall facing.

Wu et al. [14] performed another study on two GRS abutments in Turner-Fairbank, Virginia. One of the abutments used strong geotextile reinforcement with an ultimate tensile strength of 70 kN/m and the second abutment used weak geotextile reinforcement with an ultimate tensile strength of 21 kN/m. After the construction of these abutments, a series of vertical loads with a 50-kPa increment were applied on a 0.91-m wide rigid sill seated near the wall facing on the top of abutments. The vertical and lateral deformations and strains in reinforcement were measured during the loading. Similar to the findings from Wu [13], the vertical and lateral deformations and strains in the reinforcement increased with the applied load. Tests showed that the ultimate bearing capacity of the abutment using the strong reinforcement was more than 900 kPa while the ultimate bearing capacity of the abutment using the weak reinforcement barely reached 400 kPa. Under the same load, the abutment using the weak reinforcement produced about twice the vertical deformation than the one using the strong reinforcement. This phenomenon was also found in the lateral deformation. The maximum strains in the strong and weak reinforcement layers were about 2.0% and 1.7% at a 200 kPa applied pressure, respectively. These measured results indicate that the stiffness of reinforcement had a significant effect on vertical and lateral deformations but a minimal effect on the strains in the reinforcement. In addition, the measured vertical earth pressures at the bottom of the abutments linearly decreased with the distance away from the facing. The method based on the 2(H):1(V) load distribution recommended could roughly estimate the vertical pressures at the bottom of the abutment.

Adams and Saunders [15] conducted a field test of GRS-IBS. The GRS-IBS used a wrapped-around facing and had a 1.5 m wall height. Settlement and lateral deformation were measured using magnetic extensometers and an inclinometer, respectively. The measured settlement of the bridge footing was smaller than 37.5 mm and the differential settlement between the bridge and its neighboring road was about 13 mm, which implied that no bump

developed at connection.

Xiao et al. [28] conducted physical model tests of vertically-loaded footings on GRS walls. They found that the ultimate bearing capacity of the footing depended on the offset distance of the footing to the wall facing (D_s), the footing size (B_f), the geogrid length (L), and the method of connection between geogrid and facing blocks. Fig. 9 shows the effect of the footing offset distance and the reinforcement length on the ultimate bearing capacity of the footing on the GRS wall. For a shorter reinforcement length (i.e., $L/H = 0.7$), there was an optimum offset distance for the ultimate bearing capacity of the footing on the GRS wall. When the footing was close to the end of the reinforcement, the footing failed due to the limited bearing capacity of the soil. For a longer reinforcement length (i.e., $L/H = 2.0$), there was no bearing capacity reduction within the reinforcement length after reaching the peak value of the bearing capacity. In addition, an increase of the footing width increased the bearing capacity of the footing. Xiao et al. [28] found that the critical failure surface could be simulated by a limit equilibrium method when the footing was close to the wall facing.

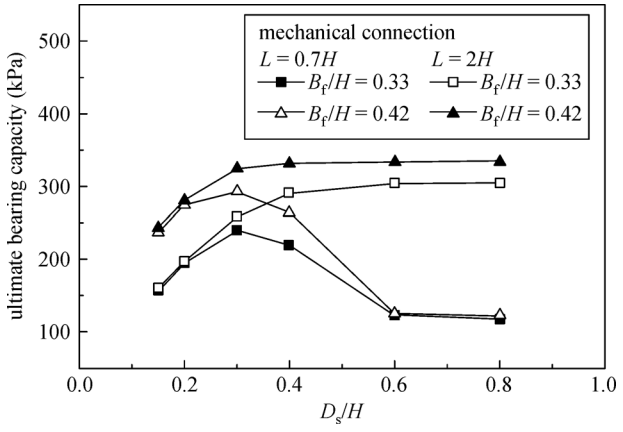

Fig. 9 Effect of footing offset distance and reinforcement length on bearing capacities of the footing on GRS walls (after Xiao et al. [28])

In addition to the field tests, Adams et al. [27] introduced the basic principles of GRS structures and proposed the methods to calculate the ultimate bearing capacity of the footing on the GRS system and the required reinforcement strength. The analytical solution was developed based on the concept of passive failure of a confined composite soil column with an apparent cohesion. The confinement by the wall facing, the geosynthetic vertical spacing, the geosynthetic tensile strength, the maximum particle size of backfill, and the friction angle of backfill contribute to the ultimate bearing capacity of the footing. The required tensile strength of the geosynthetic reinforcement depends on the lateral earth pressure, the geosynthetic vertical spacing, the maximum particle size of backfill, and the friction angle of backfill. In addition, Adams et al. [27] proposed a method to estimate the lateral deformation of the wall facing based on the assumption that the volume change in the GRS composite is zero. This assumption led to a relationship that the lateral strain is half of the vertical strain.

Numerical studies were also conducted to investigate the performance of GRS structures. Limited numerical studies have been done so far on the GRS walls. All these studies used the finite element method. Most of the numerical analyses were done in 2D under working or ultimate strength conditions. The GRS structures analyzed had the following parameters: (1) wall height ranging from 1.9 m to 6.7 m, (2) reinforcement length ranging from 1.4 m to 5.0 m, (3) reinforcement spacing ranging from 0.2 m to 0.4 m, (4) geologic cap or hardening soil model, (5) mostly linearly elastic geosynthetic elements, (6) fully-bonded interface between geosynthetic and soil, (7) use of interface between backfill soil and facing block and interface between facing blocks, and (8) compressible or incompressible foundation. In all the reviewed GRS-IBS studies, no seismic condition was considered.

4 Hybrid GRR walls

Hybrid GRR walls are a wall type between typical GRR walls and GRS walls. In this new wall system, there are long and strong primary reinforcement and short and weak secondary reinforcement. Leshchinsky [21] stated that the use of secondary reinforcement between primary reinforcement could mitigate the problems resulting from the large vertical spacing of primary reinforcement in GRR walls. Leshchinsky [21] indicated that the inclusion of secondary reinforcement can result in the following benefits: (1) a reduction in connection load for primary reinforcement, (2) an increase in internal stability from lower layers of secondary reinforcement, (3) an improved compaction near the wall facing, and (4) an alleviation of down-drag behind the wall facing. Leshchinsky and Vulova [22] employed a numerical method to investigate the influence of secondary reinforcement on the performance of hybrid walls. Their study illustrated that the inclusion of secondary reinforcement could reduce the connection load in the primary reinforcement, increase wall internal stability, and change the failure mode from connection failure to compound failure. Han and Leshchinsky [23] and Leshchinsky et al. [24] used a limit equilibrium method to investigate the effect of secondary reinforcement on the behavior of GRR walls and demonstrated the reduction of the maximum tensile force and the connection force by secondary reinforcement. In addition to these theoretical and numerical analyses of the hybrid GRR wall, Jiang et al. [6,25] performed field tests to investigate the effect of the secondary reinforcement on the performance of hybrid GRE walls with instrumentation as

shown in Fig. 10. The results from the field tests confirmed that the secondary reinforcement could reduce the lateral deformation of wall facing, reduce the connection force, and the maximum tensile force in the primary reinforcement. Jiang et al. [6,25] also found that the secondary reinforcement changed the lateral earth pressure distribution to a more uniform one.

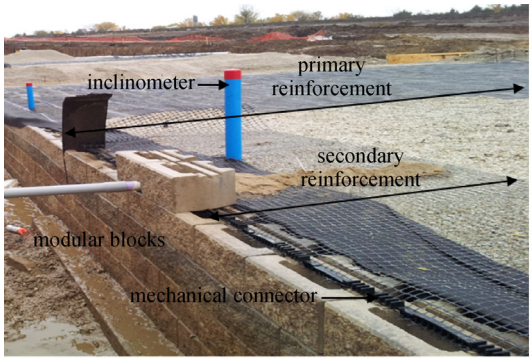

Fig. 10 Instrumented wall section with secondary reinforcement

5 Summary

This paper reviews the recent advances in geosynthetic-reinforced retaining (GRR) walls including piles in GRR walls, geosynthetic-reinforced soil (GRS) walls, and hybrid GRR walls and summarizes the main research activities and findings. Below is a brief summary:

(1) A pile in a GRR wall at a larger distance away from the back of wall facing could carry more lateral load than that at a closer distance. Group piles deflected more than a single pile when they are at the same distance from the back of wall facing, which demonstrates a reduction in lateral load capacity in the pile group. To avoid a group effect from neighboring piles, pile spacing should be larger than the width of influence by an individual pile. The backfill with a higher modulus required smaller pile spacing to reduce the group effect.

(2) Under the lateral load from piles, the deflection of wall facing increased with the wall height and the maximum deflection of the wall facing occurred at the wall top. The deflection of wall facing at the bottom of wall was small due to the base restraint. Maximum strains occurred in the geogrid near piles.

(3) The lateral earth pressure at the back of wall facing increased with the lateral load on the pile and was between the at-rest and passive earth pressure states. The lateral load on the pile resulted in an increase of lateral earth pressure in the central region of the wall and a decrease in the adjacent region.

(4) Under an applied footing load, the maximum lateral deformation of the wall facing first happened in the upper part of the wall and then moved to the middle of wall height when the footing load increased. A clear bulge happened in the middle area of the wall facing when the footing pressure reached to the ultimate bearing capacity.

(5) Under a footing load on the GRS pier, the measured strains in each instrumented geotextile were uniformly distributed and the maximum strains in the geotextile occurred in the area near the middle of the wall facing. The stiffness of reinforcement had a significant effect on the vertical and lateral deformations.

(6) The ultimate bearing capacity of a footing on the GRS wall depended on the distance of the footing to the wall facing, the footing width, the reinforcement spacing and length, the confinement by the wall facing, and the backfill properties. A larger reinforcement spacing required a higher tensile strength of the reinforcement.

(7) The numerical studies on GRS walls show that the geosynthetic stiffness had a significant effect on the performance of the GRS bridge abutment, the geosynthetic spacing had a moderate effect, and the fill friction angle had the least effect.

(8) Secondary reinforcement in hybrid GRE walls reduces the connection force for primary reinforcement and the lateral deformation of the wall facing, increased internal stability, improved compaction near the wall facing, and mitigated the down-drag force behind the wall facing.

Acknowledgements This research was partially sponsored by the China-US Joint Research Project (No. 2016YFE0105800) under the National Scientific and Technological Innovation Plan of the Ministry of Science and Technology of China.

References

1. Allen T M, Christopher B R, Elias V, DiMaggio J. Development of the Simplified Method for Internal Stability Design of Mechanically Stabilized Earth Walls. Report No. WA-RD 513.1, Washington State Department of Transportation, Olympia, Washington, 2001
2. Abu-Hejleh N, Zornberg J G, Wang T. Monitored displacements of a unique geosynthetic-reinforced walls supporting bridge and approaching roadway structures. In: Proceedings of the 80th Annual Meeting, Transportation Research Board, 07-11 January, Washington, D.C. (CD-ROM), 2001
3. Yang G, Zhang B, Lv P, Zhou Q. Behaviour of geogrid reinforced soil retaining wall with concrete-rigid facing. Geotextiles and Geomembranes, 2009, 27(5): 350–356
4. Pierson M C, Parsons R L, Han J, Brennan J J. Laterally loaded shaft group capacities and deflections behind an MSE wall. Journal of Geotechnical and Geoenvironmental Engineering, 2011, 137(10): 882–889
5. Allen T M, Bathurst R J. Design and performance of a 6.3 m high block-faced geogrid wall designed using the K-stiffness method. Journal of Geotechnical and Geoenvironmental Engineering, 2014, 142(2): 12–20
6. Jiang Y, Han J, Parsons R L, Cai H. Field Monitoring of MSE Walls to Investigate Secondary Reinforcement Effects. Final Report for

the KTran Research Program, Kansas Department of Transportation, 2015
7. AASHTO. AASHTO LRFD Bridge Design Specifications, 7th Ed., Washington, DC, 2014
8. Han J. Principles and Practice of Ground Improvement. John Wiley & Sons, Hoboken, New Jersey, 2015, 432
9. Pierson M C, Parsons R L, Han J, Brown D A, Thompson R W. Capacity of Laterally Loaded Shafts Constructed behind the Face of a Mechanically Stabilized Earth Block Wall. Final Report for the KTran Program, Kansas Department of Transportation, 2008, 237
10. Huang J, Bin-Shafique S, Han J, Rahman M S. Modelling of laterally loaded drilled shaft group in mechanically stabilised earth wall. Proceedings of the ICE-Geotechnical Engineering, 2014, 167 (4): 402–414
11. Huang J, Han J, Parsons R L, Pierson M C. Refined numerical modeling of a laterally-loaded drilled shaft in an MSE wall. Geotextiles and Geomembranes, 2013, 37: 61–73
12. Huang J, Parsons R L, Han J, Pierson M C. Numerical analysis of a laterally loaded shaft constructed within an MSE wall. Geotextiles and Geomembranes, 2011, 29(3): 233–241
13. Wu J T H. Revising the AASHTO Guidelines for Design and Construction of GRS Walls. Report No. CDOT-DTD-R-2001-16, Colorado Department of Transportation, 2001, 148
14. Wu J T H, Lee K Z Z, Helwany S B, Ketchart K. Design and Construction Guidelines for Geosynthetic-Reinforced Soil Bridge Abutments with a Flexible Facing. Report No. 556, National Cooperative Highway Research Program, Washington, DC, 2006
15. Adams M T, Saunders S A. Upper Ouachita National Wildlife Refuge GRS Abutments for Replacement Bridges. Presentation, FHWA, 2007
16. Vennapusa P, White D J, Klaiber F W, Wang S, Gieselman H. Geosynthetic Reinforced Soil for Low-Volume Bridge Abutments. Report No. IHRB Project TR-621, Iowa Department of Transportation, Ames, 2012
17. Bloser S, Shearer D, Corradini K, Scheetz B. Geosynthetically Reinforced Soil-Integrated Bridge Systems (GRS-IBS) Specification Development for PennDOT Publication 447. Publication No. 447 (10-14), Pennsylvania Department of Transportation, 2012
18. Alzamora D. Massachusetts Every Day Counts Showcase on GRS-IBS. Presentation, FHWA, 2013
19. Budge A, Dasenbrock D, Mattison D, Bryant G, Grosser A, Adams M, Nicks J. Instrumentation and early performance of a large grade GRS-IBS wall. ASCE Geo-Congress 2014, Geo-characterization and Modeling for Sustainability, 2014
20. Warren K A, Whelan M J, Hite J, Adams M. Three year evaluation of thermally induced strain and corresponding lateral end pressures for a GRS IBS in Ohio. ASCE Geo-Congress 2014, Geo-characterization and Modeling for Sustainability, 2014
21. Leshchinsky, D. Alleviating connection load. Geotechnical Fabrics Report, 34–39, 2000
22. Leshchinsky D, Vulova C. Numerical investigation of the effects of geosynthetic spacing on failure mechanisms of MSE block walls. Geosynthetics International, 2001, 8(4): 343–365
23. Han J, Leshchinsky D. General analytical framework for design of flexible reinforced earth structures. Journal of Geotechnical and Geoenvironmental Engineering, 2006, 132(11): 1427–1435
24. Leshchinsky D, Kang B J, Han J, Ling H I. Framework for limit state design of geosynthetic-reinforced walls and slopes. Transportation Infrastructure Geotechnology, 2014, 1(2): 129–164
25. Jiang Y, Han J, Parsons R L, Brennan J J. Field instrumentation and evaluation of modular-block MSE walls with secondary geogrid layers. Journal of Geotechnical and Geoenvironmental Engineering, 2016, 142(12): 05016002
26. Pierson M, Parsons R, Han J, Brennan J. Capacities and Deflections of Laterally Loaded Shafts Behind Mechanically Stabilized Earth Wall. Transportation Research Record, 2009, 2116: 62–69
27. Adams M T, Nicks J E, Stabile T, Wu J T H, Schlatter W, Hartmann J. Geosynthetic Reinforced Soil Integrated Bridge System, Synthesis Report. Report No. FHWA-HRT-11-027, Federal Highway Administration, McLean, VA, 2011
28. Xiao C, Han J, Zhang Z. Experimental study on performance of geosynthetic-reinforced soil model walls on rigid foundations subjected to static footing loading. Geotextiles and Geomembranes, 2016, 44(1): 81–94